Journal of Magnetism and Magnetic Materials 322 (2010) 2948–2955

Contents lists available at ScienceDirect

Journal of Magnetism and Magnetic Materials

journal homepage: www.elsevier.com/locate/jmmm

A two-particle exchange interaction model

Julia Lyubina*, Karl-Hartmut Müller, Manfred Wolf, Ullrich Hannemann

IFW Dresden, Institute for Metallic Materials, P.O. Box 270016, D-01171 Dresden, Germany

ARTICLE INFO

Article history:
Received 24 March 2010
Received in revised form
22 April 2010
Available online 13 May 2010

Keywords:
Magnetization reversal
Exchange interaction
Noncollinear behaviour
Permanent magnet
Nanocomposite
δM-plot

ABSTRACT

The magnetisation reversal of two interacting particles was investigated within a simple model describing exchange coupling of magnetically uniaxial single-domain particles. Depending on the interaction strength W, the reversal may be cooperative or non-cooperative. A non-collinear reversal mode is obtained even for two particles with parallel easy axes. The model yields different phenomena as observed in spring magnets such as recoil hysteresis in the second quadrant of the field-magnetisation-plane, caused by exchange bias, as well as the mentioned reversal-rotation mode. The Wohlfarth's remanence analysis performed on aggregations of such pairs of interacting particles shows that the deviation $\delta M(H_m)$ usually being considered as a hallmark of magnetic interaction vanishes for all maximum applied fields H_m not only at $W=0$, but also for sufficiently large values of W. Furthermore, this so-called δM-plot depends on whether the sample is ac-field or thermally demagnetised.

1. Introduction

The hysteresis behaviour of a system consisting of magnetic particles is greatly complicated by the interactions between them. This problem has been treated in literature since a long time [1–3]. It has been shown by Brown [4] that mean-field approaches can yield erroneous results, especially when calculating switching fields and coercivity based on them. Exact solutions are possible only in a few simple cases, and have been obtained e.g. for the case of dipole interaction between two identical uniaxial particles [4,5]. Skomski and Sellmayer [6] obtained switching fields for a system consisting of two particles coupled by a simple interaction, such as also assumed in this study. However, no analysis has been performed whether further reversal modes may exist additionally to those obtained from an extrapolation of the behaviour of non-interacting particles as described in the Stoner–Wohlfarth model [7]. For non-interacting single-domain particles according to the Stoner–Wohlfarth model, a reversible rotation of the magnetisation additionally to irreversible switching occurs only if the easy axes are not parallel to the applied magnetic field. In this paper, the appearance of a non-collinear reversal mode, similar to modes observed in exchange-spring magnets, will be demonstrated on the basis of the simple two-particle interaction model. It will be shown that due to the interaction between the two particles, a reversible magnetisation rotation mode may exist even if the easy axes are parallel to each other and to the applied field.

Henkel plots [8,9] or δM-plots [10] are often used for a qualitative analysis of magnetic interaction from experimental magnetic hysteresis data. Such an analysis is based on a short but ingenious paper by Wohlfarth, where different types of remanent magnetisation of minor (or recoil) hysteresis loops are compared [11]. In this study, conclusions from the Wohlfarth's remanence analysis will be tested using exact demagnetisation curves of the interaction model mentioned above, which is described in Section 2 in detail.

2. Model and critical fields

Let us consider two single-domain particles with a uniaxial anisotropy and of identical volume V. The particles are presumed to have parallel magnetic easy axes (Fig. 1), but different first anisotropy constants K_1 and K_2 (here always $K_1 \geq K_2 > 0$) and to be coupled by a ferromagnetic exchange coupling (magnetostatic interaction being anisotropic in its nature as well as higher order anisotropy constants are not considered here at all). The ferromagnetic exchange within the particles is assumed to be infinite (rigid particle). After applying a sufficiently strong magnetic field along the easy axes (*e.a.*) the system becomes saturated, both moments are aligned along their *e.a.* ($\theta_1=\theta_2=0$). If a reverse field $H>0$ is applied in the direction parallel to the easy axes, magnetisation reversal starts at some critical (switching) field. In our approach, the ferromagnetic exchange coupling is described by $E_W \sim -W(\cos\theta_1\cos\theta_2+\sin\theta_1\sin\theta_2\cos(\varphi_1-\varphi_2))$,

* Corresponding author at: IFW Dresden, Helmholtzstr. 20, 01069 Dresden, Germany. Tel.: +49 351 4659 347; fax: +49 351 4659 490.
E-mail address: j.lyubina@ifw-dresden.de (J. Lyubina).

0304-8853/$ - see front matter © 2010 Elsevier B.V. All rights reserved.
doi:10.1016/j.jmmm.2010.05.011

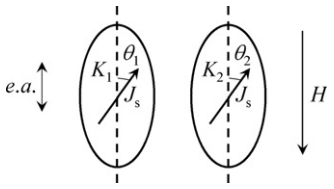

Fig. 1. Two interacting single-domain particles with parallel easy axes (*e.a.*) and different anisotropy constants in a demagnetising field $H>0$.

where $W>0$ is the coupling constant and φ_i is the azimuth angle. For any θ_1 and θ_2 choosing $\varphi_1-\varphi_2\neq 0$ results in an increase of the exchange energy. Thus, during magnetisation reversal, the two moments and the applied field form a common plane and it is sufficient to minimize the following (free)-energy density:

$$\frac{E}{V}=K_1\sin^2\theta_1+K_2\sin^2\theta_2+J_sH\cos\theta_1+J_sH\cos\theta_2-W\cos(\theta_1-\theta_2) \tag{1}$$

where J_s is the spontaneous polarisation (for simplicity, assumed to be identical for both particles). The angles θ_1 and θ_2 vary between 0 and π. For fixed values of H, the equilibrium conditions

$$\frac{\partial E}{\partial\theta_1}=K_1\sin 2\theta_1-J_sH\sin\theta_1+W\sin(\theta_1-\theta_2)=0 \tag{2a}$$

$$\frac{\partial E}{\partial\theta_2}=K_2\sin 2\theta_2-J_sH\sin\theta_2-W\sin(\theta_1-\theta_2)=0 \tag{2b}$$

yield three obvious solutions

(I) $\theta_1=\theta_2=0$;
(II) $\theta_1=0$ and $\theta_2=\pi$;
(III) $\theta_1=\theta_2=\pi$ (3)

The stability of these solutions in an increasing reverse field has to be investigated. Moreover, stable solutions different from those given by Eq. (3) also need to be examined.

Additionally to equilibrium conditions in Eq. (2), the stability conditions

$$\frac{\partial^2E}{\partial\theta_1^2}\frac{\partial^2E}{\partial\theta_2^2}-\left(\frac{\partial^2E}{\partial\theta_1\partial\theta_2}\right)^2>0 \tag{4a}$$

$$\frac{\partial^2E}{\partial\theta_2^2}>0 \tag{4b}$$

have to be satisfied simultaneously for a solution to be stable. Obviously, the trivial solution (III) is reached for sufficiently large H and is then stable. For the initial state (I) with $\theta_1=\theta_2=0$, stability is given by the following restrictions for H:

$$H>H_{\uparrow\uparrow}^{(1)}\equiv\frac{K_1+K_2+W}{J_s}+\sqrt{\frac{(K_1-K_2)^2+W^2}{J_s^2}} \tag{5}$$

$$H<H_{\uparrow\uparrow}^{(2)}\equiv\frac{K_1+K_2+W}{J_s}-\sqrt{\frac{(K_1-K_2)^2+W^2}{J_s^2}} \tag{6}$$

$$H<H_{\uparrow\uparrow}^{(3)}\equiv\frac{2K_2+W}{J_s} \tag{7}$$

whereas for the solution (II) the restrictions read

$$H<H_{\uparrow\downarrow}^{(1)}\equiv\frac{K_1-K_2}{J_s}+\sqrt{\frac{(K_1+K_2)^2-2W(K_1+K_2)}{J_s^2}} \tag{8}$$

$$H>H_{\uparrow\downarrow}^{(2)}\equiv\frac{K_1-K_2}{J_s}-\sqrt{\frac{(K_1+K_2)^2-2W(K_1+K_2)}{J_s^2}} \tag{9}$$

$$H>H_{\uparrow\downarrow}^{(3)}\equiv\frac{-2K_2+W}{J_s} \tag{10}$$

where the indices $\uparrow\uparrow$ and $\uparrow\downarrow$ denote the magnetisation direction within the two particles $\theta_1=\theta_2=0$ and $\theta_1=0$, $\theta_2=\pi$, respectively (see Fig. 1). The stability regions are determined taking into account that on the initial state, a reverse increasing field H is applied. For the initial state (I) $\theta_1=\theta_2=0$, the fields $H_{\uparrow\uparrow}^{(2)}\le H_{\uparrow\uparrow}^{(3)}<H_{\uparrow\uparrow}^{(1)}$ and, therefore, the $\uparrow\uparrow$ state becomes unstable at $H=H_{\uparrow\uparrow}^{(2)}$. Note that for a sufficiently strong interaction $W>W_{NC}$, where

$$W_{NC}=(K_1+K_2)/2 \tag{11}$$

Eqs. (8) and (9) following from Eq. (4b) have no real solutions, i.e. in this case the state $\uparrow\downarrow$ is never realised during magnetisation reversal. For $W<W_{NC}$ and because of $H_{\uparrow\downarrow}^{(3)}<H_{\uparrow\downarrow}^{(2)}<H_{\uparrow\downarrow}^{(1)}$, the stability region of the state (II) $\uparrow\downarrow$ is $H_{\uparrow\downarrow}^{(2)}<H<H_{\uparrow\downarrow}^{(1)}$. Because of the existence of the solution (II), it is not trivial in which way the magnetisation reversal occurs. In principle, it might be possible that with increasing H the initial state, which becomes unstable at $H=H_{\uparrow\downarrow}^{(2)}$, is driven into the state $\uparrow\downarrow$ (stable up to $H_{\uparrow\downarrow}^{(1)}$).

There exist several interesting limits of W. The first one, $W\ll K_1$-K_2, representing the case of weak interactions, yields the critical fields

$$H_{\uparrow\uparrow}^{(1)}=\frac{2K_1+W}{J_s}\text{ and }H_{\uparrow\uparrow}^{(2)}=\frac{2K_2+W}{J_s}\quad(\theta_1=\theta_2=0) \tag{12}$$

$$H_{\uparrow\downarrow}^{(1)}=\frac{2K_1-W}{J_s}\text{ and }H_{\uparrow\downarrow}^{(2)}=\frac{-2K_2+W}{J_s}\quad(\theta_1=0;\ \theta_2=\pi) \tag{13}$$

From Eq. (12) and $K_1>K_2$, it follows that the instability in the parallel alignment of the moments of the particles is determined by the critical field $H_{\uparrow\uparrow}^{(2)}(=H_{\uparrow\uparrow}^{(3)})$. For applied fields below $H_{\uparrow\uparrow}^{(2)}$, no reversal occurs. For $H_{\uparrow\uparrow}^{(2)}<H_{\uparrow\downarrow}^{(1)}$ or $W<K_1$-K_2 with increasing H the state $\uparrow\downarrow$ may be realised. Then, as the applied field is increased further, the particles reverse in a non-cooperative way at different fields $H_{\uparrow\uparrow}^{(2)}=(2K_2+W)/J_s$ and $H_{\uparrow\downarrow}^{(1)}=(2K_1-W)/J_s$ by either a two-step jump or non-cooperative rotation, as is discussed in detail below.

All the reversal modes may be distinguished as cooperative and non-cooperative: the *non-cooperative reversal* leads to switching of one of the particles and the second particle remains in the initial state, while the term *cooperative reversal* merely means that both particles reach their final reversed state together. Thus, the cooperative reversal may proceed by both coherent, i.e. it occurs by a simultaneous rotation of the two moments through equal angles in the same direction, as well as by an incoherent rotation. This distinction is based on the stability regions of the states $\uparrow\uparrow$ and $\uparrow\downarrow$. From the analysis based on Eqs. (2)–(4), no conclusions can be made concerning the state beyond the instability. Further, as pointed out by Brown [4], in order to prove that the reversal is coherent, a study of the dynamic behaviour at finite angles is necessary. This will not be done here.

As mentioned for strong interactions, $W>W_{NC}$, the state $\uparrow\downarrow$ is not realised and the state $\uparrow\uparrow$ becomes unstable if H exceeds the smallest field among those given by Eqs. (5)–(7), i.e. $H_{\uparrow\uparrow}^{(2)}$. In the limit of strong interactions, the reversal is cooperative.

Magnetisation reversal is cooperative and coherent, if the anisotropies of both particles are equal, $K_1=K_2=K$. The stability analysis yields

$$H_{\uparrow\uparrow}^{(1)}=\frac{2K+2W}{J_s}\text{ and }H_{\uparrow\uparrow}^{(2)}=\frac{2K}{J_s}\quad(\theta_1=\theta_2=0) \tag{14}$$

$$H_{\uparrow\downarrow}^{(1)}=\frac{2K}{J_s}\sqrt{1-\frac{W}{K}}\quad(\theta_1=0;\ \theta_2=\pi) \tag{15}$$

The instability of the $\theta_1=\theta_2=0$ state is determined by $H^{(2)}_{\uparrow\uparrow}$ of Eq. (14), since the upper limit for the stable region of the state $\uparrow\downarrow$ given by Eq. (15) is below those in Eq. (14). In the model considered here, the ferromagnetic interaction constant W is positive and the particles will reverse at the common switching field $H^{(2)}_{\uparrow\uparrow}=2K/J_s$, independent of the interaction strength.

3. Magnetic phase diagram

In Section 2, the critical fields and stability regions of the magnetisation states (I)–(III) given in Eq. (3) have been derived. Knowledge of these fields is important, but not sufficient for predicting the way, in which the magnetisation reversal occurs. The existence of additional non-trivial solutions, additional to those given by Eq. (3), cannot be excluded. In this section, magnetic phase diagrams and energy surfaces are examined, analytically as well as numerically, for particular parameters and related to the discussed effects. The results are given on the basis of stability diagrams, which show the fields $H^{(1)}_{\uparrow\downarrow}$, $H^{(2)}_{\uparrow\downarrow}$ and $H^{(2)}_{\uparrow\uparrow}$ in a H–W plane, and thereby determining the stability regions. A variety of the magnetic phases and types of possible magnetisation reversal processes follow from the discussion, given below for two examples. The magnetisation $J_s=1.43$ T for both particles and $K_1=7.0$ MJ/m^3, which correspond to the room temperature saturation magnetisation and anisotropy constant of the $L1_0$ FePt phase, respectively [12], and two different K_2 were selected, while W has been varied.

3.1. Case 1: $K_1=7.0$ MJ/m^3 and $K_2=1.0$ MJ/m^3

For relatively strong K_2 with respect to K_1, the stability diagram is also a magnetic phase diagram, i.e. it predicts the mechanism by which magnetisation reversal occurs. For the case $K_1=7.0$ MJ/m^3 and $K_2=1.0$ MJ/m^3 this follows from the detailed analysis of energy surfaces (not shown here). For these parameters, the critical field contours (Eqs. (6), (8) and (9)) are plotted in dependence on W (Fig. 2). This figure shows the regions of cooperative and non-cooperative reversal for particular J_s, K_1 and K_2 values and the states, which are realised after applying the reverse field H. In the shaded area in Fig. 2 both configurations, $\uparrow\downarrow$ and $\uparrow\uparrow$, are stable. Let us start from the saturated state ($\theta_1=\theta_2=0$) in zero external field. As the reverse field $H>0$ is applied and increased, the particles remain in their initial state until the reverse field intensity reaches $H^{(2)}_{\uparrow\uparrow}$. When the interaction is small ($W<W_{WCM}$), where

$$W_{WCM}=\frac{K_1\sqrt{5K_2^2+4K_1K_2}-K_2(K_1+2K_2)}{K_1+K_2} \tag{16}$$

an increase of the external field above $H^{(2)}_{\uparrow\uparrow}$ will lead to non-cooperative jump, i.e. the particle with smaller anisotropy K_2 will reverse, whereas the high-anisotropy particle K_1 will remain in its initial direction. As the external field reaches the stability limit $H^{(1)}_{\uparrow\downarrow}$ (Eq. (8)), the high anisotropy particle will reverse as well. The switching fields for both particles are modified by the interaction: as the interaction strength W increases, the field $H^{(2)}_{\uparrow\uparrow}$, at which the smaller anisotropy particle reverses, increases, whereas smaller fields are required to reverse the high-anisotropy particle. When the interaction strength exceeds some limit (in the case considered $W>W_{NC}$), cooperative reversal is observed, as the state $\uparrow\downarrow$ is never stable for these parameters.

As a matter of course, the magnetisation state of these two single-domain particles depends not only on interaction strength, anisotropy and external magnetic fields, but also upon the magnetic prehistory of the sample. For instance, in the limit of strong interactions (when the reversal is cooperative), starting from the reversed state ($\theta_1=\theta_2=\pi$) and reducing the reverse field to zero again, will not bring the system to the state $\theta_1=\theta_2=0$, but the spins will of course remain in the $\theta_1=\theta_2=\pi$ configuration. The same is true for the case of small and moderate interaction strength ($W<W_{NC}$, non-cooperative reversal), if the reverse field has exceeded $H^{(1)}_{\uparrow\downarrow}$. In these cases, the stability analysis has to be done for that initial state and a starting increasing field of opposite direction.

Consequently, for small and moderate interaction strength $W<W_{WCM}$, reducing the reverse field, which reached a value above $H^{(2)}_{\uparrow\uparrow}$ but below $H^{(1)}_{\uparrow\downarrow}$, to zero again will result in the appearance of recoil hysteresis: the particle with smaller anisotropy will return to the initial state $\theta_2=0$ not in the field $H^{(2)}_{\uparrow\uparrow}$ (upper limit of the shaded area in Fig. 2), but in the smaller one $H=H^{(2)}_{\uparrow\downarrow}$ (lower limit of the shaded area in Fig. 2). This type of hysteresis is also reflected in the behaviour of the energy profile

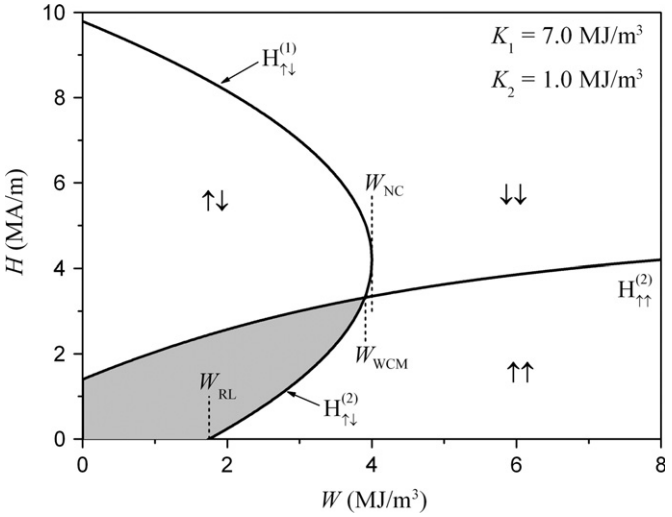

Fig. 2. Stability diagram for two interacting single domain particles showing the regions of cooperative and non-cooperative reversal for $K_1=7.0$ MJ/m^3, $K_2=1.0$ MJ/m^3 and $J_s=1.43$ T. The upper boundary of the shaded area limits the stability of the $\uparrow\uparrow$ configuration when increasing H from zero up to $H^{(2)}_{\uparrow\uparrow}$, whereas the lower one limits the $\uparrow\downarrow$ stability region for decreasing H provided the reverse field was below $H^{(1)}_{\uparrow\downarrow}$. The critical fields $H^{(1)}_{\uparrow\downarrow}$, $H^{(2)}_{\uparrow\downarrow}$ and $H^{(2)}_{\uparrow\uparrow}$ and interaction strength W_{RL}, W_{WCM} and W_{NC} are given in the text.

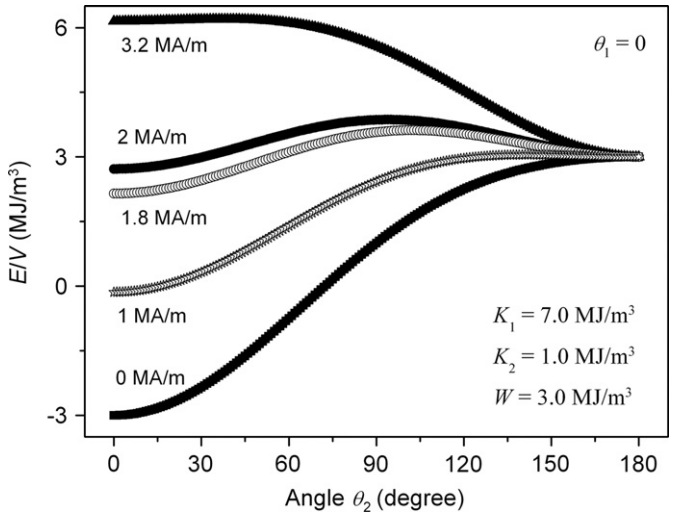

Fig. 3. Energy profile versus rotation angle of the low anisotropy particle (θ_2) for increasing reverse field H from 0 to 2.0 and to 3.2 MA/m (closed symbols) and subsequently decreasing reverse field to 1.8 and to 1.0 MA/m (open symbols). The parameters used in the calculation are: $J_s=1.43$ T, $K_1=7.0$ MJ/m^3, $K_2=1.0$ MJ/m^3 and $W=3.0$ MJ/m^3. θ_1 has been fixed to zero for the considered fields.

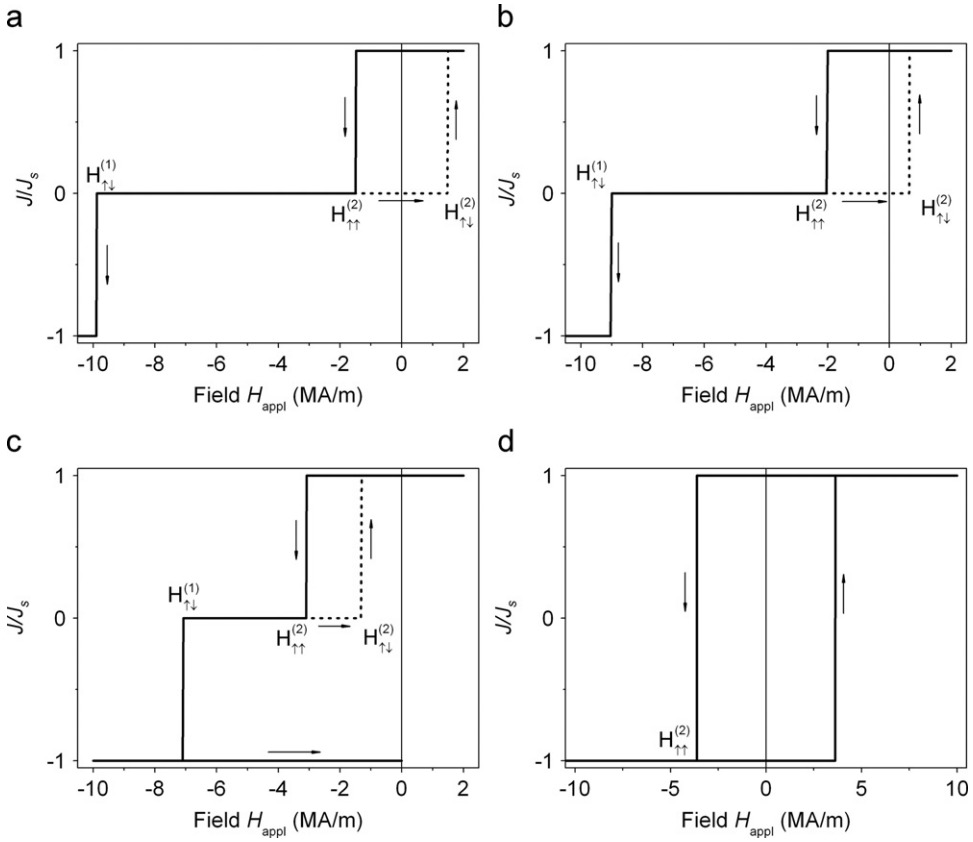

Fig. 4. Demagnetisation curves of two particles interacting according to Eq. (1) for $K_1=7.0$ MJ/m^3, $K_2=1.0$ MJ/m^3, together with certain minor recoil curves for (a) vanishing interaction, $W=0$, (b) $0<W<W_{RL}$, W=1MJ/m^3, (c) $W_{RL}<W<W_{WCM}$, W=3MJ/m^3 and (d) $W>W_{NC}$, W=5MJ/m^3. According to the definition in Eq. (1) the applied field is $H_{appl}=-H$.

plots (Fig. 3). For the given interaction strength $W=3$ MJ/m^3 ($<W_{WCM}$), the particles remain in the initial state $\theta_1=\theta_2=0$ for reverse fields up to $H=H^{(2)}_{\uparrow\uparrow}\approx 3$ MA/m, as can be inferred from the existence of the energy barriers for fields below 3 MA/m. In a reverse field of 3.2 MA/m, the magnetisation of the particle with smaller anisotropy reverses. Since this field is below the field, at which the high-anisotropy particle switches, $H^{(1)}_{\uparrow\downarrow}$, the latter will not rotate, i.e. for the considered reverse fields θ_1 is always zero. Subsequent reduction of the reverse field will bring the system into the initial state $\theta_1=\theta_2=0$, not at the critical field $H^{(2)}_{\uparrow\uparrow}$, but in a smaller field equal to $H^{(2)}_{\uparrow\downarrow}\approx 1.4$ MA/m (Fig. 2), and thus for 1 MA/m the barrier in Fig. 3 has disappeared.

In terms of the hysteresis loop, this situation is illustrated in Fig. 4(a)–(c) and corresponds to the so-called recoil-loop measurements. In the absence of interactions, $W=0$, for an applied field larger than the switching field of the low-anisotropy particle ($H^{(2)}_{\uparrow\uparrow}$), but below the switching field of the high-anisotropy particle ($H^{(1)}_{\uparrow\downarrow}$), the low-anisotropy particle reverses, while the high-anisotropy particle remains in the initial state (Fig. 4(a)). If the reverse field is subsequently reduced, the low anisotropy particle follows its own hysteresis loop. In order to reverse the low anisotropy particle, application of the positive field equal to $2K_2/J_s$ is required. This means, that in the absence of interactions, $W=0$, for applied fields below the switching field of the high-anisotropy particle a minor loop arising only from the low-anisotropy particle hysteresis is observed. Interaction between the particles shifts the minor loop to higher reverse fields producing the recoil loops (Fig. 4(b) and (c)), as follows from Fig. 2. According to the model, the recoil loop area decreases with increasing interaction strength, and it vanishes in the limit of strong interactions (compare Figs. 2 and 4). Interaction between the particles modifies the fields $H^{(2)}_{\uparrow\uparrow}$ and $H^{(1)}_{\uparrow\downarrow}$. Nevertheless, the low anisotropy particle switches irreversibly. For non-vanishing interaction, but $W<W_{RL}$ with

$$W_{RL}=\frac{2K_1K_2}{K_1+K_2} \tag{17}$$

the low anisotropy particle is reversed back in positive $H_{appl}=-H^{(2)}_{\uparrow\downarrow}>0$ (Fig. 4(b)), the branch $H^{(2)}_{\uparrow\downarrow}$ below the abscissa in Fig. 2, not shown there. If the interaction is in the range $W_{RL}<W<W_{WCM}$, the complete recoil loop shifts to the second quadrant, i.e. to negative H_{appl} (Fig. 4(c)). For strong enough interactions, $W>W_{NC}$, the minor loop disappears and the two particles switch in unison (Fig. 4(d)).

3.2. Case 2: $K_1=7.0$ MJ/m^3 and $K_2=0.1$ MJ/m^3

The stability diagram for the case of $K_1=7.0$ MJ/m^3 and $K_2=0.1$ MJ/m^3, i.e. a second particle with weak anisotropy shown in Fig. 5 indicates that there exists a wide critical region $W_{WCM}<W<W_{NC}$, where neither the state $\theta_1=\theta_2=0$ nor the state $\theta_1=0$; $\theta_2=\pi$ is stable.

The question arises, whether the $\theta_1=\theta_2=\pi$ state is stable. But inspecting the energy surface curves revealed a more complex behaviour: a further reversal mode, additional to the transition between the states given by Eq. (3), has been observed (see Fig. 6): with increasing reverse field above $H^{(2)}_{\uparrow\uparrow}$, the particles do not switch but start to tilt by different angles with respect to the easy direction. As a guide for the eye, the direction of the magnetisation of both particles at a given reverse field is also schematically shown in Fig. 6. Provided the reverse field is below $H^{(2)}_{\uparrow\downarrow}$, the rotation is fully reversible. The reverse field $H=H^{(1)}_{\uparrow\downarrow}$ promotes the irreversible switching of both particles.

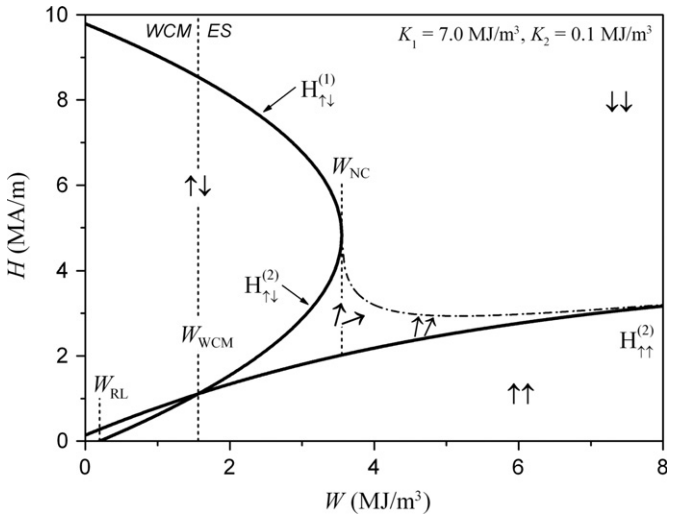

Fig. 5. Stability diagram for two interacting single domain particles showing weakly coupled (*WCM*) and exchange-spring (*ES*) reversal mode regions for $K_1=7.0$ MJ/m^3, $K_2=0.1$ MJ/m^3 and $J_s=1.43$ T. The boundary between the noncollinear reversal mode and $\theta_1=\theta_2=\pi$ is indicated by a dot-dashed line. The critical fields $H^{(1)}_{\uparrow\downarrow}$, $H^{(2)}_{\uparrow\downarrow}$ and $H^{(2)}_{\uparrow\uparrow}$ and interaction strengths W_{RL}, W_{WCM} and W_{NC} are given in the text.

Thus, depending on the interaction strength, three major reversal modes can be distinguished: (1) weakly coupled magnet (*WCM*) region, where the low- and high-anisotropy particles behave almost independently, (2) region with exchange-spring behaviour (*ES*) for sufficiently strong coupling and (3) high-anisotropy-particle dominated region, where the low- and high-anisotropy particles switch in unison (Fig. 5).

In the *ES* regime, the low- and high-anisotropy particles rotate non-collinearly. As the reverse field increases, the tilting angle θ_2 of the low anisotropy particle increases faster than that of the high anisotropy particle (Fig. 7). Whereas θ_2 increases steadily with H, the angle θ_1 first increases and then relaxes to zero, again if θ_2 goes to π, if $W_{WCM}<W<W_{NC}$. The particles are thus driven into the state $\uparrow\downarrow$, but during this process the high anisotropy particle is perturbed by the rotation of the low anisotropy particle.

With increasing interaction strength, higher reverse fields are required to switch the low anisotropy particle. However, when the interaction exceeds some limit, given by $W>W_{NC}$, the high anisotropy particle does not relax to the initial state, but the non-collinear reversible rotation is followed by the irreversible switching of both particles ($W=4.0$ MJ/m^3 in Fig. 7). Thus, also in the *ES* regime, the switching of both particles can be either cooperative or non-cooperative depending on the interaction strength. For $K_1=7.0$ MJ/m^3 and $K_2=0.1$ MJ/m^3, the cooperative switching by the *ES* non-collinear mechanism is observed for the interaction strength $W>W_{NC}$. The boundary limiting the stability of the non-collinear mode is sketched in Fig. 5. It is determined numerically using the equilibrium conditions in Eq. (2). This boundary continuously approaches the stability limit $H^{(2)}_{\uparrow\uparrow}$ with increasing W, since the deviation of the magnetisation from *e.a.* and the angle $(\theta_2-\theta_1)$ decreases with increasing interaction. For $W\to\infty$, the magnetisation reversal is collinear.

Fig. 8 shows demagnetisation curves as a function of interaction strength. In the limit of weak interactions $W<W_{WCM}$ ($W=1$ MJ/m^3), the particles switch almost independently. With increasing interaction $W>W_{WCM}$, the demagnetisation curve is not rectangular in shape and one can distinguish the first critical field, at which non-collinear reversible rotation starts, and the second critical field, at which the high anisotropy particle switches irreversibly. The switching field for irreversible rotation decreases dramatically with increasing the interaction strength. Depending on the interaction strength, the reversal is non-cooperative ($W_{WCM}<W<W_{NC}$, e.g. $W=3$ MJ/m^3) or cooperative ($W>W_{NC}$, e.g. $W=4$ MJ/m^3). In the limit of very strong interactions (e.g. $W=8$ MJ/m^3), the demagnetisation curve is largely rectangular, with a single critical field, being substantially smaller than that of the non-interacting high-anisotropy particle. However, the coherent magnetisation reversal is expected only for $W\to\infty$, where the particles behave as a rigid magnet.

4. Wohlfarth's remanence analysis

In order to obtain information on magnetic interaction in a material from experimental hysteresis data Wohlfarth [11] derived the simple relationship

$$2J_R(H_m)+J_D(H_m)-J_R=0 \tag{18}$$

being valid for an assembly of non-interacting magnetically uniaxial single-domain particles. In Eq. (18) $J_R(H_m)$ is the remanent magnetisation of the sample measured after a positive field H_m had been applied to and subsequently removed from the sample, which was thermally or ac-field demagnetised (however—not dc-field demagnetised). $J_R=J_R(\infty)$ is the common remanence of the system. The remanent magnetisation $J_D(H_m)$ is acquired after the sample has been saturated in a large positive field, and then a field $-H_m$ had been applied and subsequently removed. Thus, deviations from Eq. (18) can be caused by (1) non-uniaxial anisotropy, (2) non-homogeneous magnetisation modes (deviating from the single-domain state) or (3) particle interaction. It should be noted that Eq. (18) holds whatever the degree of orientation (texture) of the easy axes and whatever the variation of the anisotropy within the assembly is. On the other hand, the validity of Eq. (18) is only a necessary condition for the sample to be a system of non-interacting magnetically uniaxial single-domain particles. Also, if the conditions for the validity of Eq. (18) are not fulfilled, the deviations from it could depend on whether the sample was thermally or ac-field demagnetised.

According to Eq. (18), the quantity

$$\delta M(H_m)=2J_R(H_m)/J_R+J_D(H_m)/J_R-1 \tag{19}$$

vanishes for the ideal case of an assembly of non-interacting magnetically uniaxial single-domain particles. Therefore, the so-called δM plots, i.e. $\delta M(H_m)$-versus-H_m-curves, have been used to analyse the deviations of the behaviour of real materials from the ideal case [8,10].

Here, we consider the δM plot for the very simple system consisting of an aggregation of independent pairs of particles described by Eq. (1). It is obvious from Figs. 2 and 4 that the δM plot completely vanishes, $\delta M(H_m)=0$, for arbitrary $H_m>0$, not only for the ideal case $W=0$, but also for $W>W_{RL}$, independent of whether the analysis started with a thermally or an ac-field demagnetised state. In the case of $W_{RL}<W<W_{WCM}$ (as in Fig. 4(c)), the recoil hysteresis has no influence on remanent states (i.e. states at $H=H_{appl}=0$) and for $W>W_{WCM}$ there is no recoil hysteresis as the pairs switch in unison. Hence, $\delta M(H_m)\neq 0$ can only appear for weak interaction $0<W<W_{RL}$.

If the system is ac-field demagnetized, it consists of pairs $\uparrow\uparrow$, $\downarrow\downarrow$, $\uparrow\downarrow$ and $\downarrow\uparrow$, each with a statistical weight of 25%. For $0<W<W_{RL}$, the values of $\delta M(H_m)$ of such a sample are non-zero only in the field range

$$-H^{(2)}_{\uparrow\downarrow}<H_m<H^{(2)}_{\uparrow\uparrow} \tag{20}$$

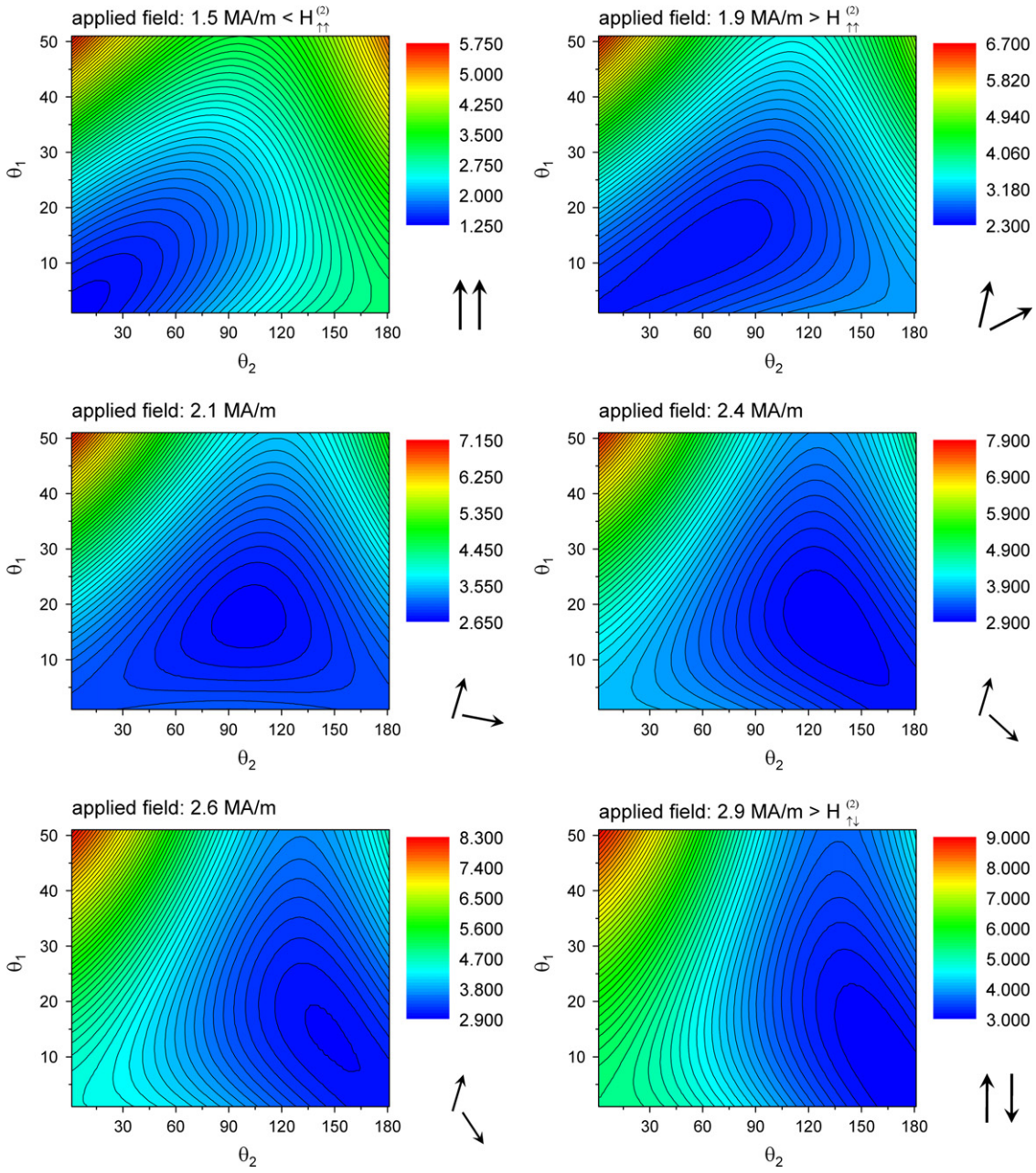

Fig. 6. Energy surface contour plots of two interacting particles for the reverse field increasing from 1.5 to 2.9 MA/m (J_s=1.43 T, K_1=7.0 MJ/m^3, K_2=0.1 MJ/m^3 and W=3.0 MJ/m^3). The magnetisation direction (θ_1, θ_2) of the two particles is given by the minimum of the energy, somewhere in the centre of the darkest blue region. Arrows show schematically the direction of the magnetisation of the particles at the corresponding reverse field.

with $H^{(2)}_{\uparrow\downarrow}$ and $H^{(2)}_{\uparrow\uparrow}$ from Eqs. (9) and (6), respectively, and has the value $\delta M(H_m)=1/2$. As an example, the δM plot corresponding to the case of Fig. 4(b) is shown in Fig. 9.

On the other hand, the detailed state of the corresponding thermally demagnetised system depends on the temperature dependencies of the material parameters J_s, K_1, K_2 and W. It can be easily shown that both types of thermally demagnetised states can appear, the one obtained also for ac-field demagnetisation (see above), whereas the other is a collection of pairs $\uparrow\uparrow$ and $\downarrow\downarrow$, each with a statistical weight of 50%. In the latter case, there is $\delta M(H_m)=0$ for all values $H_m>0$.

The novel non-collinear magnetisation mode discussed in Section 3.2 is reversible and has no influence on states at $H_{appl}=0$, and consequently it does not modify the δM plot. Note that in the exchange-spring regime, the pairs $\uparrow\downarrow$ and $\downarrow\uparrow$ are not stable in $H_{appl}=0$.

5. Conclusions

The influence of magnetic interaction between different types of ferromagnetic particles on the magnetisation reversal in permanent magnets has been investigated using a very simple two-particle model. Information on the reversal mechanisms and critical fields, at which the reversal takes place has been described by magnetic phase diagrams in terms of magnetic field, interaction strength and anisotropy strengths. Although the anisotropy axes of both particles have been chosen parallel to each other and

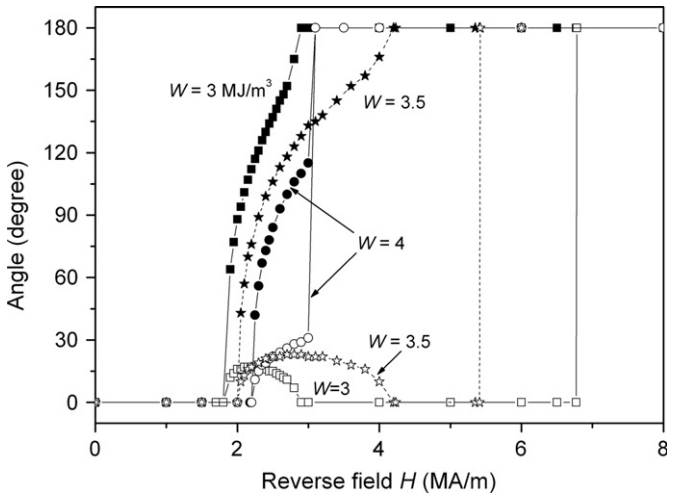

Fig. 7. Calculated angles θ_1 (open symbols) and θ_2 (closed symbols) as a function of the reverse field for various interaction strength W (K_1=7.0 MJ/m^3, K_2=0.1 MJ/m^3, J_s=1.43 T).

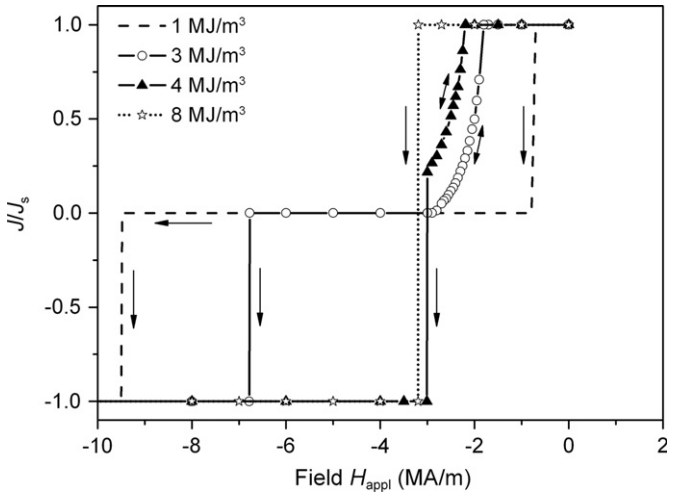

Fig. 8. Calculated demagnetisation curves of two interacting particles for different values of the interaction strength W (K_1=7.0 MJ/m^3, K_2=0.1 MJ/m^3 and J_s=1.43 T). According to the definition in Eq. (1) H_{appl}= -H.

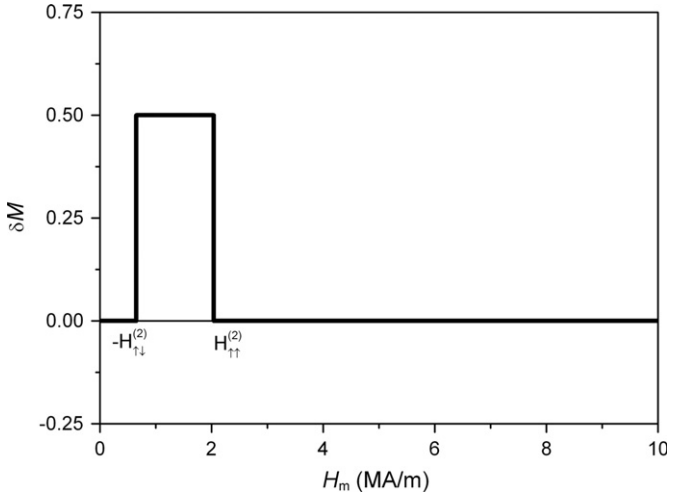

Fig. 9. δM plot according to Eq. (19) for an ac-field demagnetised assembly of independent pairs of particles described by Eq. (1), with the parameters of Fig. 4(b).

to the magnetic field non-collinear reversal modes have been obtained. Similar modes are known from non-textured nanocomposite exchange-spring magnets [13–15]. Depending on the interaction strength, the reversal may be cooperative or non-cooperative also in the regime of this kind of exchange-spring behaviour (see Fig. 7). Non-collinear reversal modes have also been observed by Fullerton et al. [16] and Amato et al. [17], where exchange-spring soft/hard layers consisting of hundreds of spins were studied using a one-dimensional discrete model qualitatively similar to Eq. (1). It is striking that here the existence of the non-collinear reversal mode can be obtained considering interactions between only two particles with parallel easy axes, thus suggesting that the exchange-spring behaviour is a very general phenomenon.

Any reversal mode, including the mentioned type of exchange-spring behaviour, is characterised by the dependence $\theta_1(H)$ and $\theta_2(H)$, which may be mapped as a curve in the θ_1–θ_2 plane. Fig. 10 summarises schematically the different characteristic modes found for the model of this study. In the case of equal anisotropy constants, a transition from the $\theta_1=\theta_2=0$ to $\theta_1=\theta_2=\pi$ state occurs by a simultaneous switching. This conclusion is made on the basis of the equilibrium Eq. (2). However, to follow the details of this reversal would require a study of the dynamic behaviour [4]. Non-cooperative switching is observed in the case of weak ($W < W_{WCM}$) or absent interaction ($W=0$). In the *ES* region, reversible magnetisation rotation is followed by an irreversible switching. Depending on the interaction strength, reversal can be either non-cooperative (*ES NC*), for $W_{WCM} < W < W_{NC}$ or cooperative (*ES C*), for $W > W_{NC}$.

Exchange spring behaviour can also be resembled by shifted recoil loops similar to that in Fig. 4(c). Such shifting caused by magnetic interaction has been proposed by Preisach [18]. Meiklejohn and Bean [19] observed such an effect for ferromagnetic particles exchange coupled to an antiferromagnet, and they designated this effect as an exchange anisotropy. If both K_2 and W are small, the closed recoil loop in Fig. 4(c) becomes narrow and close to the field axis similar to the reversible curves in Fig. 8 and to the recoil loops observed in exchange spring materials [12,13,20].

This very simple but exactly solvable model could successfully be used to answer general questions concerning the Wohlfarth's remanence analysis: although the δM plot for an assembly of non-interacting uniaxial single-domain particles yields $\delta M(H_m)\equiv 0$ for both, thermally and ac-field demagnetised samples, the deviations of δM from zero may be different for the two types of demagnetising and δM can even be zero for finite (in particular strong) interaction between the particles.

The model investigated in this study can be extended to more general cases such as different spontaneous magnetisations

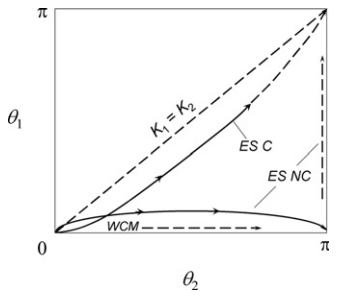

Fig. 10. Schematic representation of possible reversal modes in a system consisting of two interacting particles. Solid lines correspond to a reversible magnetisation rotation, dashed lines represent irreversible switching (a jump of at least one particle). Reversal in the *ES* regime is noncooperative (*ES NC*) for $W_{WCM} < W < W_{NC}$ and cooperative (*ES* C) for $W > W_{NC}$.

(or volumes) of the two particles, negative values of the interaction parameter W or different directions of the two easy axes.

Acknowledgement

The authors are grateful to O. Gutfleisch and L. Schultz for continuous scientific support.

References

[1] L. Neel, C.R. Ac, Science 224 (1947) 1550.
[2] I.S. Jacobs, C.P. Bean, Phys. Rev. 100 (1955) 1060.
[3] E.P. Wohlfarth, Proc. R. Soc. London A 232 (1955) 208.
[4] W.F. Brown, in: Magnetostatic Principles in Ferromagnetism, Amsterdam, North-Holland, 1962.
[5] W. Chen, S. Zhang, H.N. Bertram, J. Appl. Phys. 71 (1992) 5579.
[6] R. Skomski, D.J. Sellmyer, J. Appl. Phys. 89 (2001) 7263.
[7] E.C. Stoner, E.P. Wohlfarth, Philos. Trans. R. Soc. London A 240 (1948) 599.
[8] P. Gaunt, G. Hadjipanayis, D. NG, J. Magn. Magn. Mater. 54-57 (1986) 841.
[9] G.W.D. Spratt, P.R. Bissell, R.W. Chantrell, E.P. Wohlfarth, J. Magn. Magn. Mater. 75 (1988) 309.
[10] P.E. Kelly, K. O'Grady, P.I. Mayo, R.W. Chantrell, IEEE Trans. Magn. 25 (1989) 3881.
[11] E.P. Wohlfarth, J. Appl. Phys. 29 (1958) 595.
[12] J. Lyubina, I. Opahle, K.-H. Müller, O. Gutfleisch, M. Richter, M. Wolf, L. Schultz, J. Phys.: Condens. Matter 17 (2005) 4157.
[13] J. Schneider, D. Eckert, K.-H. Müller, A. Handstein, H. Mühlbach, H. Sassik, H.R. Kirchmayr, Mater. Lett. 9 (1990) 201.
[14] E.F. Kneller, IEEE Trans. Magn. 27 (1991) 3588.
[15] M. Solzi, M. Ghidini, G. Asti, Macroscopic magnetic properties of nanostructured and nanocomposite systems, in: H.S. Nalwa (Ed.), Magn. Nanostruct., American Scientific, Stevenson Ranch, CA, 2002, p. 123.
[16] E.E. Fullerton, J.S. Jiang, M. Grimsditch, C.H. Sowers, S.D. Bader, Phys. Rev. B 58 (1998) 12193.
[17] M. Amato, M.G. Pini, A. Rettori, Phys. Rev. B 60 (1999) 3414.
[18] F. Preisach, Z. Phys 94 (1935) 277.
[19] W.H. Meiklejohn, C.P. Bean, Phys. Rev. 105 (1957) 904.
[20] R.W. McCallum, J. Magn. Magn. Mater. 299 (2006) 472.